Available online at www.sciencedirect.com
SCIENCE DIRECT
Thermochimica Acta 440 (2006) 132–140
thermochimica acta
www.elsevier.com/locate/tca

Melting and glass transitions in paraffinic and naphthenic oils

J-F. Masson *, G.M. Polomark, S. Bundalo-Perc, P. Collins

Institute for Research in Construction, National Research Council of Canada, Ottawa, Ont., Canada K1A OR6

Received 4 May 2005; received in revised form 20 October 2005; accepted 1 November 2005
Available online 15 December 2005

Abstract

Naphthenic and paraffinic oils were analyzed by modulated differential scanning calorimetry (MDSC). The results showed several improvements in the analysis of thermal properties when compared with standard DSC. The glass transition temperature (T_g), the enthalpy relaxation at T_g, and the melting endotherms could be deconvoluted, and reversible melting could be identified. This allowed for an easier interpretation of the thermal properties of the oils. With MDSC, the T_gs in mineral oils were found to coincide with endothermic enthalpy relaxation, which is generally regarded as a melting endotherm with standard DSC. A decrease in heat capacity after T_g was attributed to the existence of rigid amorphous material. From Δc_p at T_g and the oil molecular weight, the number of repeat units in the oil chains was estimated at less than 20. The T_g of a hypothetical pure aromatic oil was found to be similar to that for petroleum asphaltenes, and that for a naphthenic oil of infinite molecular weight to be similar to that of petroleum resins.

Keywords: Differential scanning calorimetry (DSC); Modulated differential scanning calorimetry (MDSC); Hydrocarbons; Naphthenic oils; Paraffinic oils; Bitumen; Cold crystallization; Enthalpy relaxation; Melting; Glass transition temperature

1. Introduction

Mineral oils and paraffinic waxes are of great technological and economic interest, partly because crystalline waxes can lead to an array of difficulties. For instance, the crystallization of paraffins can lead to the clogging of pipelines during the transportation of paraffinic crude oils [1]; in roadway bitumens, crystallization may reduce the adhesion to aggregates [2]. Waxes also affect viscosity [3], thus limiting the use of oils in many applications.

Since the late 1960s and early 1970s, thermal analysis, and differential scanning calorimetry (DSC) in particular, has been used to characterize petroleum products (readers familiar with petroleum derivatives, but unfamiliar with DSC, are referred to the Glossary). DSC was used to study the glass transition temperature (T_g) and crystallization in bitumen [4,5], oils [6] and waxes [7]. Noel and Corbett [5] first established that the T_g of bitumen depended on its source and that "waxy" and "non-waxy" bitumens could be distinguished based on the DSC profiles. Upon heating, "waxy" bitumens were found to show exothermic cold crystallization and endothermic melting, both of which were reported to arise from the lighter bitumen fraction, the saturates. Giavarini and Pochetti [7] later observed two endotherms in paraffinic waxes, whereas they observed a single broad endotherm in microcrystalline (non-paraffinic) waxes. It is thus generally considered that endotherms in petroleum products arise from paraffins, or alkanes. However, it was recently demonstrated that the endotherm size in DSC is not necessarily proportional to the saturates content [8] and that the ordering of aromatic rings may also contribute to the endotherm [9].

DSC is commonly used to determine crystallinity because it is rapid and more convenient than wet chemical methods that require solvents for the extraction of crystallizing waxes. However, the DSC method consistently provides greater crystallinity values than the wet chemical method [10]. The difference is usually attributed to the crystallization of methylene segments in aromatic compounds not extracted by solvents [10], but it could also arise from the overlap of underlying transitions that enlarge the endotherm. Such transitions could be a second endotherm from the isotropization of aromatic rings, organized in a mesophase [9,11], or a second T_g [9].

The analysis of oils and petroleum products in general has yet to benefit from the latest advances in DSC, namely modulated DSC (MDSC), which has been used advantageously on some

* Corresponding author. Tel.: +1 613 993 2144; fax: +1 613 952 8102.
E-mail address: jean-francois.masson@nrc.gc.ca (J-F. Masson).

0040-6031/$ – see front matter.
doi:10.1016/j.tca.2005.11.001

Table 1
Oil characteristics

	Method[a]	Naphthenic			Paraffinic	
		N100	N200	N2000	P70	P150
Composition (%)	D2007					
Saturates		68	61	53	93	82
Aromatics		31	38	45	6	17
Polars		0.4	0.7	2	0.1	1.0
Asphaltenes		<0.1	<0.1	<0.1	<0.1	<0.1
Carbon type (%)	D2140					
Paraffinic		42	44	51	62	71
Naphthenic		49	46	26	37	27
Aromatic		9	10	13	1	2
Molecular weight	D2502	290	340	415	318	570

[a] ASTM method number.

n-alkanes [12], bitumen [11] and its fractions [9]. In this paper, MDSC is used to characterize naphthenic and paraffinic oils. The method resolves overlapping transitions in these oils, including T_g, enthalpy relaxation, cold crystallization and melting. It is shown, amongst other results, that melting enthalpies from MDSC are smaller than those from standard DSC, which may help reconcile the crystallinity measurements from calorimetry and other methods [10,13].

2. Experimental section

2.1. Materials and methods

Three naphthenic and two paraffinic oils were obtained from Ergon Inc. of Jackson, MS, USA. The composition and characteristics of the oils are shown in Table 1. The ASTM standard test [14–16] results were supplied by Ergon.

For MDSC, the heating and cooling experiments were performed between −110 and 50 °C, at a linear heating or cooling rate of 3 °C/min, a modulation period of 60 s and a modulation amplitude of ±0.47 °C. The specific heat capacity at T_g was measured from the area of the T_g peak on the derivative curve. Details are found elsewhere [9,11]. When the figures show an arrow on the abscissa, the curves were shifted for easier comparison, e.g. |← 0.06 W/g →|.

3. Results and discussion

3.1. Naphthenic oils

Fig. 1 shows the DSC results from the lightest of the naphthenic oils (N100). Upon heating, the heat flow shows a rapid decrease between −100 and −60 °C, before it levels again. The interpretation of such a curve depends much on the baseline, as three baselines (A–C) can be drawn. Baseline A drawn straight from the heat flow below −80 °C leads to a large endotherm and excludes the possibility of a T_g. Baseline B, an extension of the heat flow between −30 and 20 °C, might be interpreted as the superposition of a small T_g and a large endotherm, whereas baseline C does the reverse. Hence, with standard (linear heat rate) DSC the interpretation of heat flow profile is ambiguous.

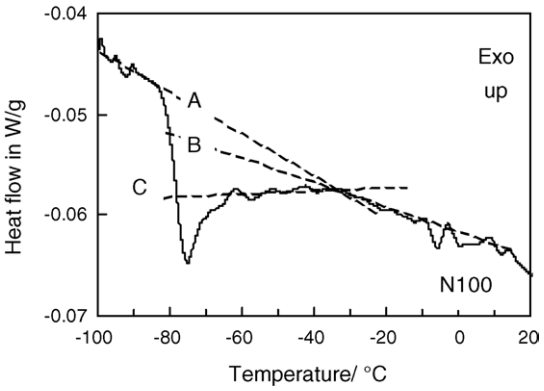

Fig. 1. DSC signal of the naphthenic oil N100 upon heating.

With MDSC, the total heat flow is deconvoluted into the reversing heat flow (RHF) and the non-reversing heat flow (NRHF) [17–19]. The total heat flow is equivalent to the standard DSC signal. The origin of the RHF and NRHF, as it pertains to hydrocarbons, has been described before [9,11,12]. In its simplest case, and at temperatures below oxidation or degradation, the RHF provides the apparent heat capacity from amorphous material and a precise measure of T_g [20]. The NRHF arises from non-reversing phenomena like evaporation, decomposition, chemical reactions, melting, crystallization and relaxation [18,19]. In some instances, however, crystallization and melting do contribute to the reversing heat flow [9,21] as a result of rapid interfacial crystallization and melting within the MDSC modulation cycle [21].

Fig. 2 shows the total, RHF and NRHF for the naphthenic oil N100. The RHF, readily converted to the specific heat capacity

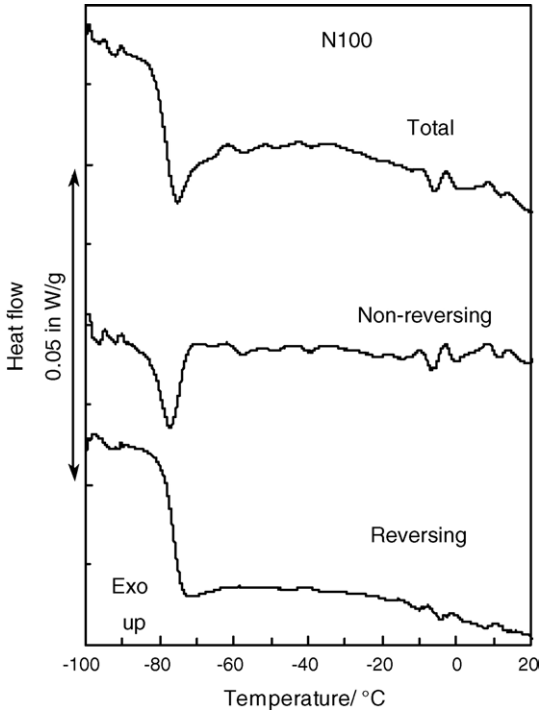

Fig. 2. Total, reversing and non-reversing heat flows from the heating of the naphthenic oil N100.

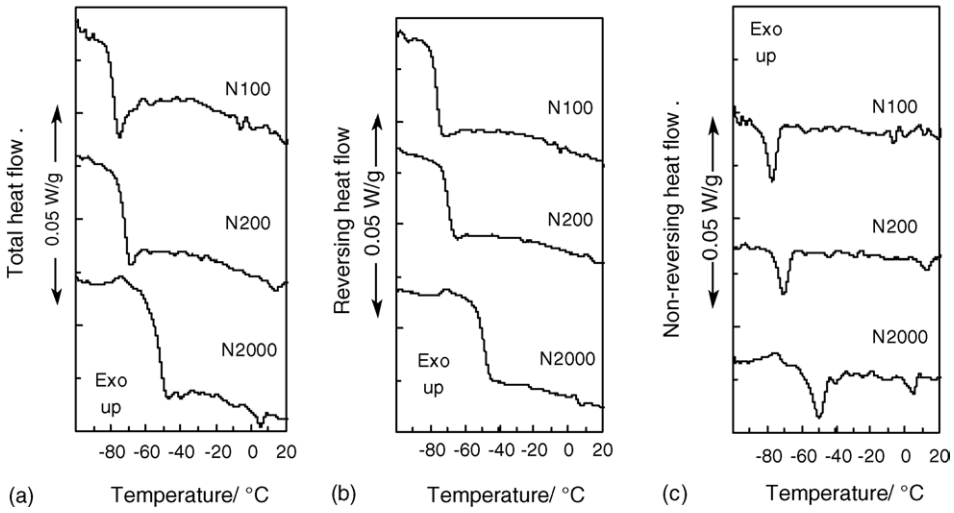

Fig. 3. Total (a), reversing (b), and non-reversing (c) heat flows from the heating of the naphthenic oils N100, N200 and N2000.

(c_p) [9], shows a large change between −93 and −70 °C due to a T_g centered at −76 °C. The deconvolution shows that baseline C in Fig. 1 was the more appropriate, although it may not have seemed the best baseline choice. Concurrent with the T_g, the NRHF shows an endothermic peak centered at −77 °C. This endotherm does not arise from melting, but from enthalpy relaxation [22], which arises from the cooperative chain motions in the T_g region [23]. Molecular mobility increases sharply at T_g, and this leads to a loss of short-range order that requires energy. This loss of order, which is an endothermic process, is reminiscent of the loss of long-range order due to melting. In standard DSC, the enthalpy relaxation is recognized as an endotherm near T_g [24]. The higher the short-range order of the amorphous material that gives rise to T_g, the greater the enthalpy relaxation and the greater the endotherm. Consequently, this enthalpy increases upon the local densification that follows annealing [23,25].

Above the enthalpy relaxation in the NRHF curve of Fig. 2, small endotherms between −20 and 20 °C are attributed to the melting of residual crystallinity. As will be seen later, this is also the temperature region where paraffinic oils show their crystallinity. The very low crystallinity of the naphthenic oil is likely due to a high concentration of poorly ordered naphthenic (cycloaliphatic) segments, which represent 49% of the carbon content (Table 1).

Fig. 3 shows the total, RHF and NRHF for three naphthenic oils. The main difference between the oils is an increase in reversing heat flow at T_g, i.e. Δc_p, and a shift in T_g to lower temperatures due to an increase in saturates content. Table 2 shows that DSC consistently placed the T_g 3–5 °C lower than MDSC. The relationship between T_g and composition will be discussed in more detail later.

There is a noteworthy positive contribution to the baseline at the end of the T_g on the RHF curve, which shows as a negative contribution to c_p (Fig. 4). Such an effect is fairly common in semi-crystalline polymers [20]. It arises from a loss of amorphous material responsible for T_g due to the stiffening effect of crystals near the amorphous material. The result is a rigid amorphous material with a T_g higher than that of the free amorphous

Table 2
T_g and Δc_p from the various mineral oils[a]

Oil	T_g		Δc_p	
	DSC	MDSC	DSC	MDSC
N100	−80	−77	0.18	0.21
N200	−74	−70	0.07	0.18
N2000	−53	−48	0.19	0.16
P70	n.d.[b]	−93, −40	n.d.	0.46[c]
P150	n.d.	−58	n.d.	0.34

[a] From the heat flow on heating.
[b] Could not be determined.
[c] For the combined T_gs.

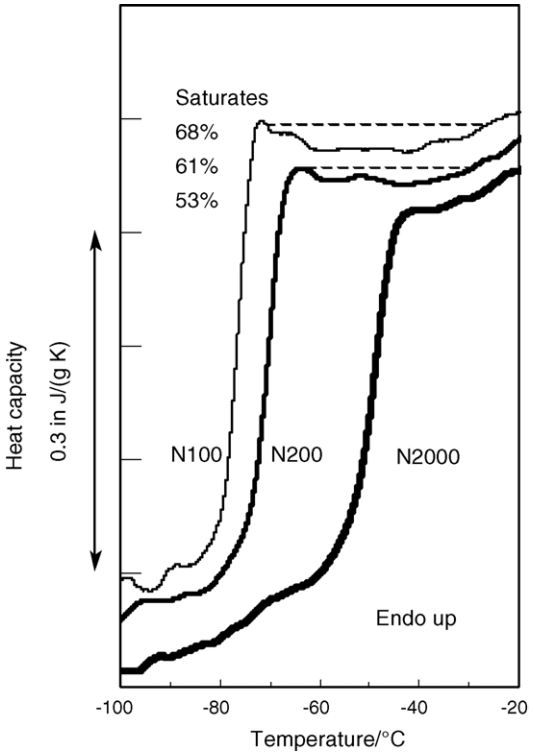

Fig. 4. Apparent c_p in the T_g region of the naphthenic oils.

material. In Fig. 4, the negative contribution to c_p was small and no second T_g could be discerned, but the negative contribution to c_p increased with the content of saturates, a fraction that is most often semi-crystalline. Little crystalline material is needed to freeze a large portion of the amorphous material into a rigid amorphous phase ([20] and references therein). The existence of such material in oils, and its effect on oil rheology, is no doubt a subject that would benefit from further work.

3.2. Paraffinic oils

DSC signals shown in Fig. 5 were obtained upon heating two paraffinic oils, P150 and P70. Such oils are known to crystallize [6]. Again, selecting a proper baseline is difficult, with baseline A likely being the most natural choice. The curves are typical of those for paraffinic oils and waxes [6] and many bitumens [26].

MDSC results on the paraffinic P150 are shown in Fig. 6. The RHF shows a T_g centered at −60 °C, whereas the NRHF indicates the existence of two endotherms with minima at −60 °C (enthalpy relaxation) and at −10 °C (melting), separated by an exotherm (cold crystallization) with a maximum at −45 °C. The deconvolution demonstrates that baseline C in Fig. 5 would have been the more appropriate, and would have led to the closest assessment of the true size of the endo- and exotherms. Interpretation of thermal events is thus facilitated by MDSC.

Above the T_g in Fig. 6, the RHF shows two small endotherms with minima at −35 and −7 °C. With bitumen, the existence of endotherms on the RHF curve was related to reversible melting and crystallization of saturated segments [9]. This reversible process normally occurs at the growth face of crystals where

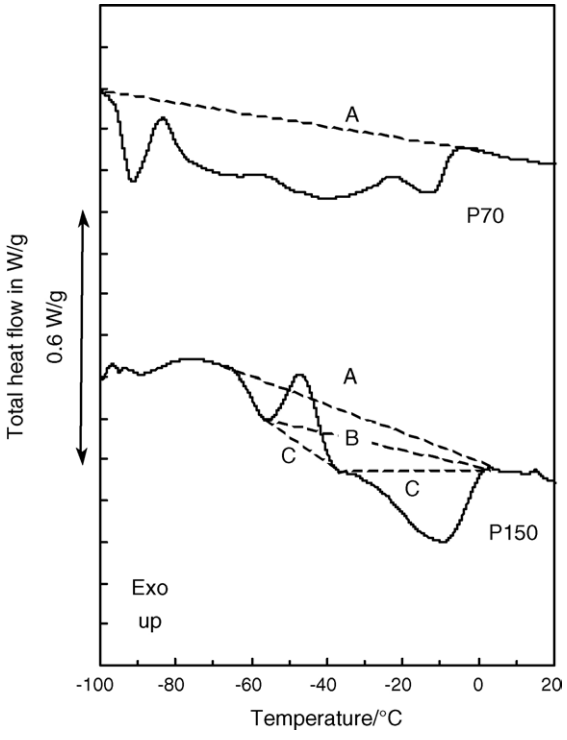

Fig. 5. Total heat flow from the heating of the paraffinic oils and some possible baselines for P150.

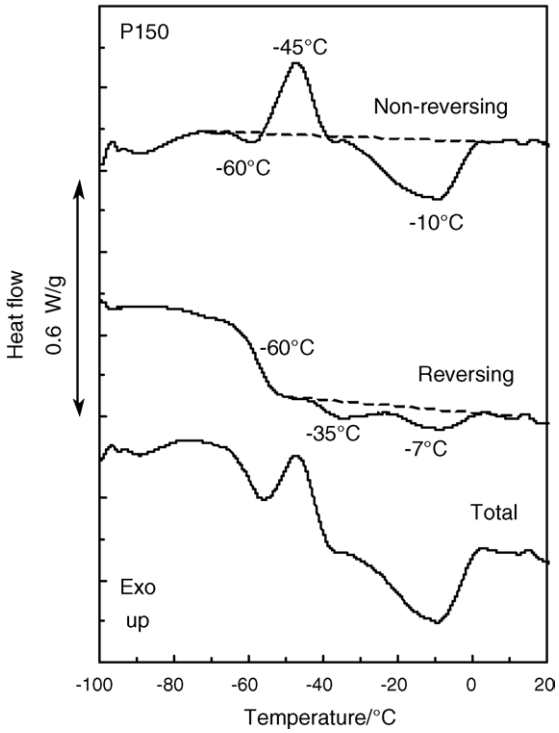

Fig. 6. Heat flow curves from the heating of paraffinic oil P150.

rapid crystallization and melting of *n*-paraffins or oligomers of low molar mass occurs [27]. In bitumen and oils, short crystallisable paraffinic segments may be anchored to higher molecular weight structures that may or may not be aromatic. Reversible melting explains the presence of endotherms on the RHF curve and the thermal hysteresis in c_p from heating and cooling runs [9] as shown in Fig. 7. Upon cooling from the liquid state, the c_p curve only shows the T_g centered around −60 °C, whereas upon heating, the presence of low molar mass paraffins allows for reversible melting between −50 and 0 °C.

Fig. 8 shows the RHF and the NRHF after the heating and cooling of the semi-crystalline P150. From the identification of the T_g region on the RHF curves, it becomes possible to correctly set a baseline and determine enthalpies on the NRHF curves. From the analysis, it is conspicuous that not all heating endotherms are from melting and that cooling exotherms are from crystallization. Upon cooling (top curve in Fig. 8), the NRHF curve shows a broad crystallization exotherm that begins at −10 °C. Its large width indicates the formation of a myriad of imperfect crystalline structures rather than large, well-shaped crystals that would have given sharp peaks upon melting. Upon continued cooling, there is a change in baseline at the onset of T_g (−52 °C) when molecular motions become very slow, to the point that crystallization cannot proceed further.

Upon heating, the NRHF signal in Fig. 8 shows that past a slight endothermic enthalpy relaxation (minimum at −60 °C), exothermic cold crystallization occurs. The ordering of crystallisable segments begins near the end of the T_g region. The crystallization occurs more readily above T_g, when diffusion is more rapid and neighbouring crystallizable segments can more easily come together. The crystallization exotherm is followed

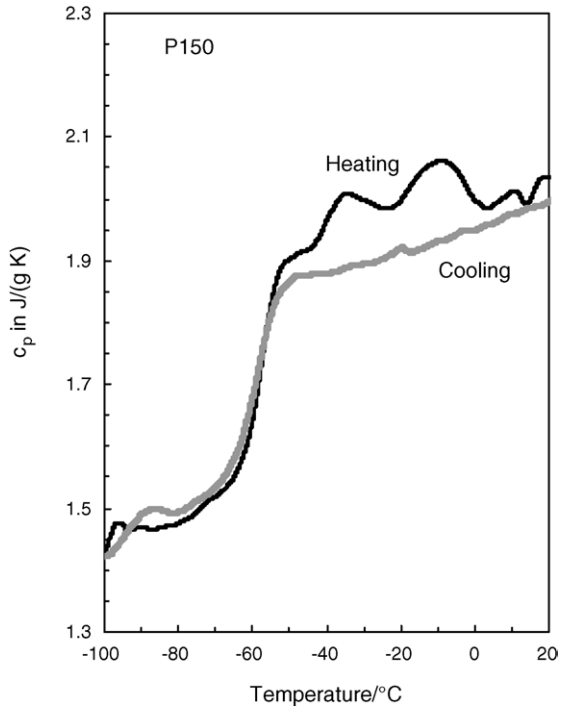

Fig. 7. Apparent c_p from the heating and cooling of paraffinic oil P150.

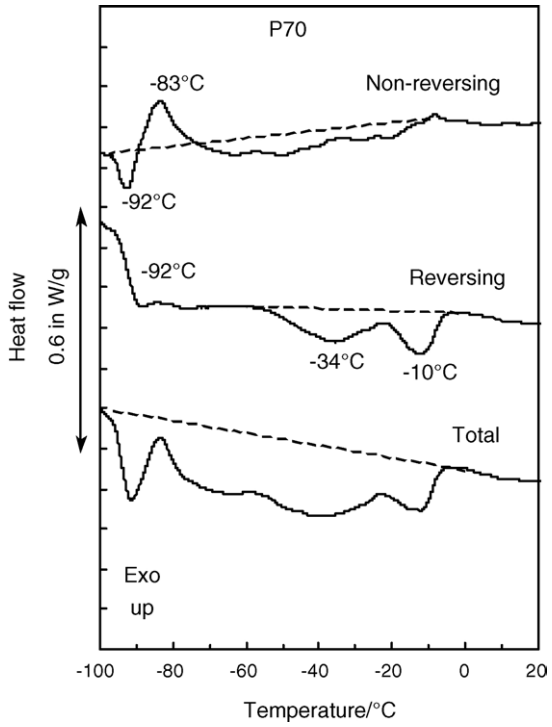

Fig. 9. Heat flow curves from the heating of the paraffinic oil P70.

by a melting endotherm, which is smaller than that indicated by the more "natural" baseline A in Fig. 5. On this basis, it may thus be concluded that crystalline contents obtained by standard DSC (Fig. 5) is overestimated because it accounts for repeating (reversible) melting and recrystallization. This may help explain the discrepancy in crystalline content measured by standard DSC and wet chemistry [10].

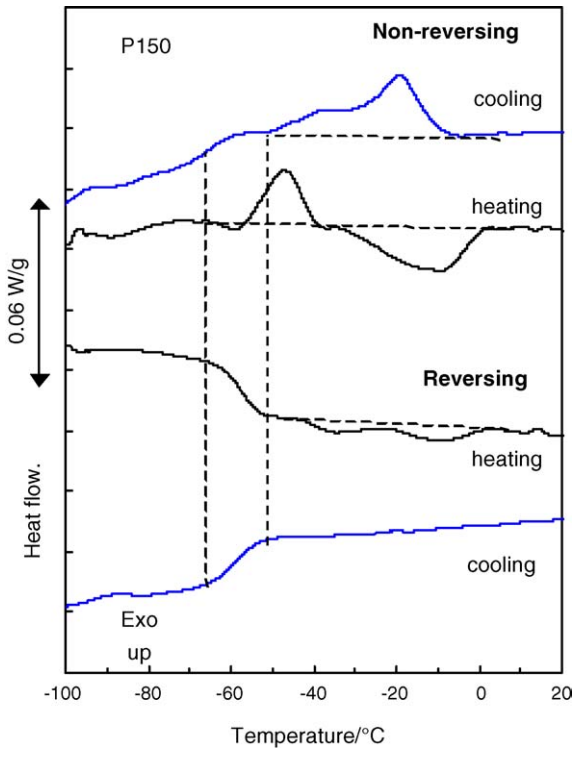

Fig. 8. Reversing and non-reversing heat flow curves obtained upon heating and cooling paraffinic oil P150.

Fig. 9 shows the MDSC results obtained upon heating another paraffinic oil, P70. Again it is conspicuous that true enthalpies are lower than estimated based on standard DSC (total heat flow). The NRHF and RHF curves show similar phenomena to those in Fig. 6 for P150. The NRHF curve in Fig. 9 shows that the enthalpies for relaxation and cold crystallization in P70 are 30–40 °C lower than in P150. The profiles of the RHF are also quite similar, except for a lower T_g and larger endotherms in P70 than in P150.

The cooling curves for P70 are shown in Fig. 10. The NRHF curve shows that exothermic crystallization at −18 °C, highlighted at the top of the figure by the dotted line, coincided with some melting, as seen at the bottom of the figure by the endothermic peak on the RHF curve. This reversible melting upon cooling was unexpected. Incomplete deconvolution of the NRHF and RHF was ruled out as the reason for the reversing endotherm, after experiments with higher modulation frequencies lead to a constant c_p, unlike the case for high molecular weight polymers [20]. This suggests that the heat released by the irreversible crystallization can be recaptured by crystals that can melt reversibly even upon cooling, when the average temperature of the oil is being reduced. This would be consistent with the ordering of low molar mass material [20,27], and as will be seen shortly, with the existence in the oils of very short oligomeric chains with repeat numbers below 20.

Cooling experiments are not often undertaken in the study of oils or bitumen. The results shown here, and those shown for bitumen fractions [9], indicate that it should be done rou-

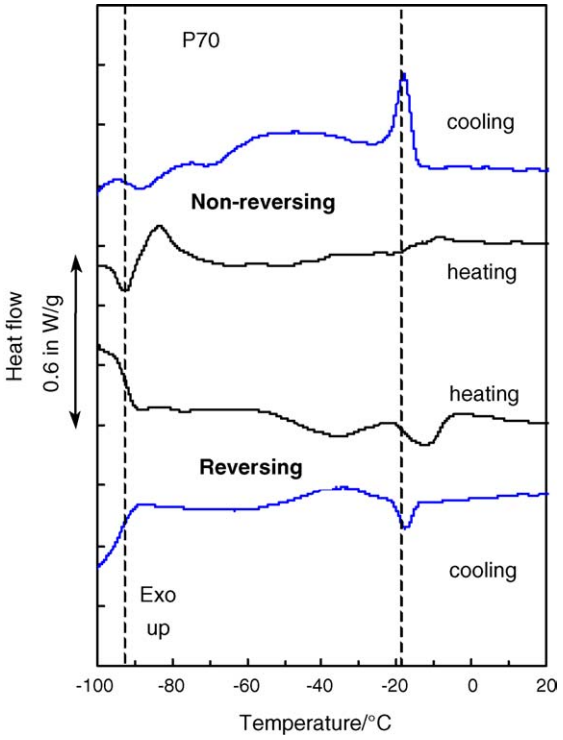

Fig. 10. Reversing and non-reversing heat flow curves obtained upon heating and cooling paraffinic oil P70.

tinely along with the heating experiments. A comparison of the c_p curves after heating and cooling clearly indicates that the seemingly endothermic melting at −34 °C in Fig. 9 is not an endotherm (Fig. 11). Both the heating and cooling curves follow each other except for the true enthalpies around −18 °C.

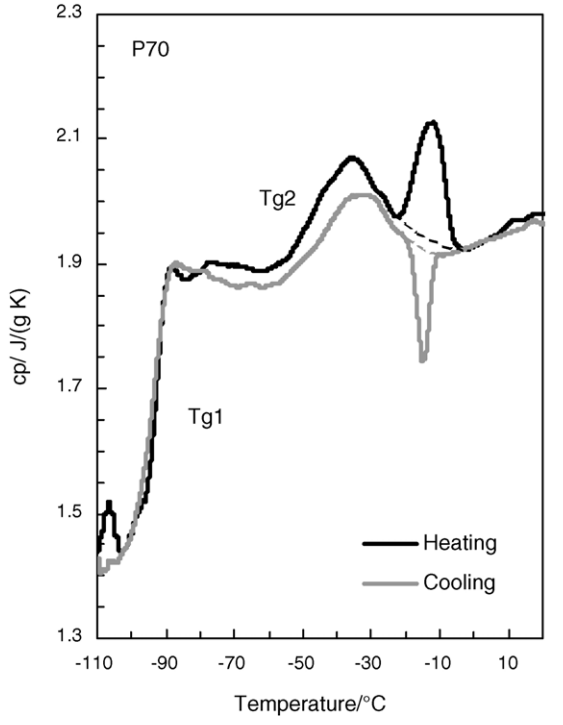

Fig. 11. Apparent c_p from the heating and cooling of paraffinic oil P70.

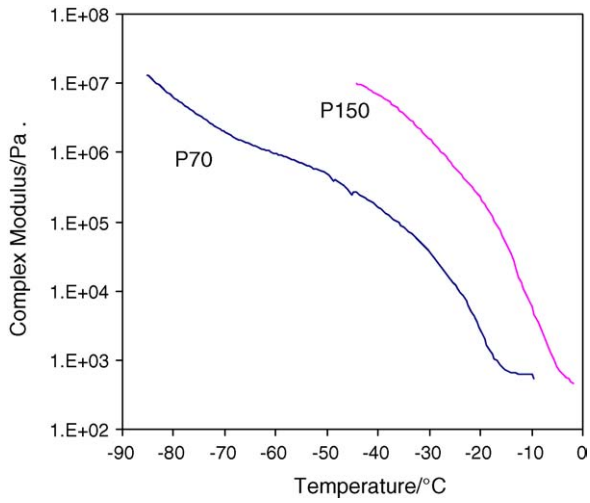

Fig. 12. Rheological curves for the paraffinic oils.

Fig. 11 demonstrates that the increase in c_p between about −60 and −30 °C was due to a second T_g.

The existence of two T_gs in the paraffinic P70 was confirmed by rheological measurements. Fig. 12 shows the complex modulus for both P150 and P70 between −90 and 0 °C. With its T_g at −58 °C and its cold crystallization below −40 °C (Fig. 6), P150 showed a high modulus below −40 °C, which decreased four orders of magnitude within 40 °C as the oil slowly liquefied (Fig. 12). In contrast, the modulus of P70 decreased to the same extent, but over 80 °C. The modulus slowly decreased with heating, and it is only beyond about –30 °C, after the second T_g (Fig. 11), that the modulus decreased rapidly.

The second T_g in P70 was not readily apparent in Fig. 6 because of a decrease in c_p past the higher T_g (Fig. 11). Earlier, a decrease in c_p was attributed the formation of a rigid amorphous phase. In this case, however, it might be attributed to the demixing of different phases [28]. Indeed, the two T_gs in P70 indicate the existence of two glassy domains of different compositions. Above the second T_g, each domain is a viscous liquid, so that two partially mixed liquids may segregate more fully from each other. The crystalline phase may impede complete segregation, if it is not part of one of the domains. Quite obviously, further work will be required to fully understanding the ordering and interactions in multi-component petroleum derivatives.

3.3. Number of repeat units in hydrocarbon chains

Like all hydrocarbon products from petroleum, the oils are mixtures. The molecular weight and polydispersity can be measured, but the number of repeat units n in the hydrocarbon chain remains undefined because of the lack of the structural regularity typical of synthetic products. In other words, hydrocarbon chains are a collection of repeat units, with each one possibly different from the next. In such a case, the value of n may be estimated from the change in heat capacity at T_g [11]. The change in the molar heat capacity for amorphous organic materials at T_g is 11 J/(mol K) [29]. The ratio of the molar heat capacity to the specific heat capacity (in J/(g K)) allows for an estimation of the

Table 3
Determination of the number of repeat units, n

Line	Parameter	N100	N200	N2000	P70	P150
A	ΔC_p at T_g ([J/(mol K)]	11	11	11	11	11
B[a]	Δc_p at T_g [J/(g K)]	0.21	0.18	0.16	0.46[b]	0.34
C (=A/B)	Average molar weight of repeat unit (g/mol)	52	61	69	24	32
D	Molecular weight (g/mol)[c]	290	340	415	318	570
E (=D/C)	Number of repeat units, n	6	6	6	13	18

[a] From MDSC.
[b] From the sum of the two T_gs.
[c] From Table 1.

relative molecular weight of the oil repeat unit (row C, Table 3), from which n can be calculated (row E, Table 3).

All the naphthenic oils show values of $n = 6$, whereas the paraffinic oils show larger values of 13 and 18. These values are well below the limit below which reversible crystallization can occur. At $n > 70$, molecular nucleation (seeding) is necessary for crystallization, but below this limit nucleation is not necessary for crystallization and it can readily occur [30]. In other words, short chains can melt and crystallize reversibly and repeatedly, which explains the reversible melting observed with the oils. The results in Table 3 are interesting on other counts: (i) n depends on the type of oil. It is larger for paraffinic oils than for naphthenic oils, which is consistent with molecular chains with small units in paraffinic oils (e.g. methylene) and chains of larger cycloalkane units in naphthenic oils [31]; (ii) the number of repeat units is constant across the naphthenic oils. Thus the increase in the molecular weight of these oils is the result of an increase in the average mass of the repeat units; (iii) in contrast, the increase in the molecular weight of the paraffinic oils is due to an increase in the average mass of the repeat units and to an increase in the number of repeat units.

3.4. T_gs in light oils and higher hydrocarbons

From the MDSC results on the paraffinic and naphthenic oils, five T_gs were obtained. This is admittedly a small data set from which to draw correlations, but this set can nonetheless help illustrate a relationship between T_gs and factors related to molecular architecture in oils and heavy hydrocarbon mixtures (e.g. bitumen), all derived from petroleum refining operations.

The T_g of an organic compound is governed by the stiffness of its molecular segments, as determined by segment polarity, aromaticity and crystallinity [32]. The T_g of the naphthenic oils studied here increased with the aromatics content, or decreased with the saturates content (Fig. 3b). From the T_gs of these naphthenic oils alone, the correlation between the T_g and the composition in saturates and aromatics (Table 1) is linear (Fig. 13). The extrapolation of this linearity to the T_gs of "pure" hydrocarbons is noteworthy. The extrapolation to a composition of 100% aromatics or 0% saturates leads to a T_g at 53–73 °C. This is coincidentally the temperature region covered by the T_g of asphaltenes [9,11]. Similarly, the extrapolation to 100% saturates or 0% aromatics leads to a T_g of −142 to −152 °C, relatively close to the T_g of long-chain n-paraffins (polyethylene) at −125 °C [33]. The low extrapolated T_g of the saturates versus polyethylene is likely a reflection of their low molecular weight and their greater segment mobility compared to long-chain paraffins. It is noteworthy that the 10–20 °C variation on the extrapolated T_gs in Fig. 13 is well within the variation in the T_g for many bitumens, which vary over 18 °C [34]. The extrapolations of the T_gs for the naphthenic oils studied and their correspondence with the T_gs of much higher molecular weight hydrocarbons thus reinforces the idea [31] that in a complex petroleum-based mixture, light and heavy hydrocarbons co-exist as a continuum.

Within the continuum, T_g can be related to molecular weight by the expression $T_g = K/M - T_{g\infty}$, where K, M, and $T_{g\infty}$ are, respectively, a constant, the molecular weight and the T_g at infinite molecular weight. This expression is commonly used for polymers [32], for which $T_{g\infty}$ is the molecular weight above which polymer chain ends no longer affect T_g. For a hypothetical heavy naphthenic oil, $T_{g\infty}$ may be obtained by a plot of T_g versus $1/M$ (Fig. 14). By extrapolation, a value of $T_{g\infty} = 14$ °C is obtained, which is close to the T_g of 20 °C for resins extracted from bitumen [9]. Consequently, naphthenic oils may be considered as reasonable low molecular weight analogs of resins extracted from bitumen or heavy oils. In other words, resins may be regarded as an ensemble of segments with molecular

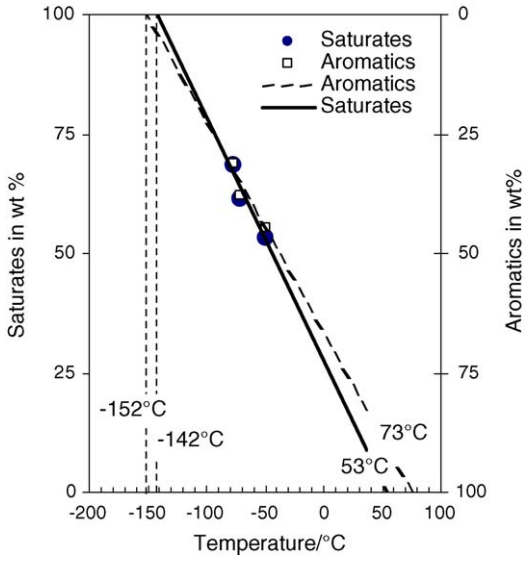

Fig. 13. Correlation between the naphthenic oil compositions and their T_g. Saturates and aromatics contents are from Table 1. Extrapolated T_gs are as indicated. See text for details.

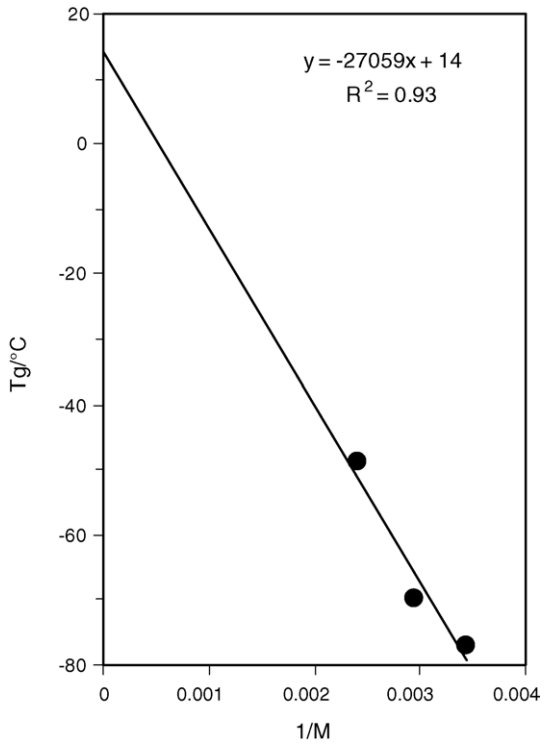

Fig. 14. Correlation between T_g and the inverse molecular weight of the naphthenic oils.

weights typical of naphthenic oils, the basis of the assembly of the naphthenic segments possibly being close to the dimerization process proposed by Michon et al. [35] to explain bitumen aging.

4. Summary and conclusion

Naphthenic and paraffinic oils were characterized by MDSC. Glass transition temperatures, and relaxation and melting endotherms could easily be identified, in contrast to regular DSC. With MDSC, it was found that each glass transition temperature (T_g) coincided with an enthalpy relaxation most often mistaken for melting in regular DSC. MDSC also allowed for the identification of reversible melting. Both the enthalpy relaxation and the reversible melting may lead to an overestimation of the DSC crystallinity in oils. The same may be expected after the analysis of other petroleum-based products.

Upon heating of the oils, MDSC allowed for the identification of a negative contribution to c_p, immediately after T_g. This was attributed to the existence of rigid amorphous material. Cooling experiments proved invaluable in determining the true nature of some features visible in the thermogram. An apparent endotherm upon heating, for instance, was found upon cooling to be a second T_g.

MDSC helped correctly measure Δc_p at T_g and locate T_g, which was 3–4 °C higher than with DSC. From Δc_p at T_g and the oil molecular weight, the size and the number of repeat units in the oil chains was calculated to be about 6 in naphthenic oils and 13 to 18 in paraffinic oils, and it was determined that the oil molecular weight was a function of both the number of repeat units in oil chains and the average mass of these units.

From the precise location of the T_gs, the composition of the oils and their molecular weights, the properties of the oils could be correlated with those of heavier hydrocarbons. The T_g of a hypothetic pure aromatic oil was similar to that for petroleum asphaltenes. The T_g of naphthenic oils of infinite molecular weight was similar to that for petroleum resins. The relationships highlighted the continuum between lighter and heavier hydrocarbons, and suggested that oils might be considered low molecular weight analogs of much heavier hydrocarbons.

References

[1] P. Singh, H.S. Fogler, N. Nagarajan, J. Rheol. 43 (1999) 1437.
[2] I. Gawel, F. Czechowski, K. Baginska, Proceedings of the Eurasphalt & Eurobitumen Congress, Strasbourg, France, May 7–10, 1996, p. 1, E&E. 5. 139.
[3] R.M. Webber, J. Rheol. 43 (1999) 911.
[4] H.J. Connor, J.G. Spiro, J. Inst. Petrol. 54 (1968) 137.
[5] F. Noel, L.W. Corbett, J. Inst. Petrol. 56 (1970) 261.
[6] F. Noel, Thermochim. Acta 4 (1972) 377.
[7] C. Giavarini, F. Pochetti, J. Therm. Anal. 5 (1973) 83.
[8] I.R. Harrison, G. Wang, T.C. Hsu, A Differential Scanning Calorimetry Study of Asphalt Binders, Report SHRP–A/URF-92-612, Strategic Highway Research Program, National Research Council, Washington, DC, 1992.
[9] J-F. Masson, G.M. Polomark, P. Collins, Energy Fuels 16 (2002) 470.
[10] D. Lesueur, J.P. Planche, P. Dumas, Bull. Labo Ponts Chaussées 229 (2000) 3.
[11] J-F. Masson, G.M. Polomark, Thermochim. Acta 374 (2001) 105–114; J-F. Masson, G.M. Polomark, Thermochim. Acta 413 (2004) 273, Erratum.
[12] J. Pak, B. Wunderlich, J. Polym. Sci. B 38 (2000) 2810.
[13] L.C. Michon, D.A. Netzel, T.F. Turner, D. Martin, J.P. Planche, Energy Fuels 13 (1999) 602.
[14] Anonymous, ASTM D2502, Standard Test Method for Estimation of Molecular Weight (Relative Molecular Mass) of Petroleum Oils From Viscosity Measurements, American Society for Standards and Testing, Barr Harbour, PA, USA.
[15] Anonymous, ASTM D2140 Standard Test Method for Carbon-Type Composition of Insulating Oils of Petroleum Origin, American Society for Standards and Testing, Barr Harbour, PA, USA.
[16] Anonymous, ASTM D2007, Standard Test Method for Characteristic Groups in Rubber Extender and Processing Oils and Other Petroleum-Derived Oils by Clay-Gel Absorption Chromatographic Method, American Society for Standards and Testing, Barr Harbour, PA, USA.
[17] M. Reading, Trends Polym. Sci. 8 (1993) 248.
[18] M. Reading, D. Ellliot, V.L. Hill, J. Therm. Anal. 40 (1993) 949.
[19] P.S. Gill, S.R. Sauerbrunn, M. Reading, J. Therm. Anal. 40 (1993) 931.
[20] B. Wunderlich, Prog. Polym. Sci. 28 (2003) 383.
[21] B. Wunderlich, I. Okazaki, K. Ishikiriyama, A. Boller, Thermochim. Acta 324 (1998) 77.
[22] B. Wunderlich, Thermal Analysis, Academic Press, New York, 1990, pp. 203–207.
[23] A. Boller, C. Schick, B. Wunderlich, Thermochim. Acta 266 (1995) 97.
[24] T. Hatakeyama, F.X. Quinn, Thermal Analysis: Fundamentals and Applications to Polymer Science, John Wiley & Sons, Chichester, 1994.
[25] I. Okazaki, B. Wunderlich, J. Polym. Sci. B 34 (1996) 2941.
[26] J.P. Planche, P.M. Claudy, J.M. Létoffé, D. Martin, Thermochim. Acta 324 (1998) 223.
[27] B. Wunderlich, Thermochim. Acta 396 (2003) 33.
[28] G. Dreezen, G. Groenickx, S. Swier, B. Van Mele, Polymer 42 (2001) 1449–1459.
[29] B. Wunderlich, Thermochim. Acta 300 (1997) 43.

[30] B. Wunderlich, A. Boller, I. Okazaki, K. Ishikiriyama, Thermochim. Acta 304/305 (1997) 125.
[31] J. Speight, The Chemistry and Technology of Petroleum, 3rd ed., Marcel Dekker, New York, 1999.
[32] A. Eisenberg, The glassy state and the glass transition, in: Physical Properties of Polymers, 2nd ed., American Chemical Society, Washington, DC, 1993, pp. 85–87.
[33] R.J. Andrews, E.A. Grulke, Glass transition temperatures of polymers, in: J. Brandup, E.H. Immergut, E.A. Grulke (Assoc. Eds.), Polymer Handbook, Wiley, New York, 1999, p. VI-206.
[34] T.F. Turner, J.F. Branthaver, DSC studies of asphalts and asphalt components, in: A.M. Usmani (Ed.), Asphalt Science and Technology, Marcel Dekker, New York, 1997 (Chapter 3).
[35] L. Michon, D. Netzel, B. Hanquet, D. Martin, J.P. Planche, Petrol. Sci. Technol. 17 (1999) 369–381.

Glossary

Amorphous material: Matter without long-range atomic or molecular order. Not crystalline.

Cold crystallization: Ordering of amorphous material into crystalline material upon heating.

Crystalline material: Matter that show a regular and repeating atomic or molecular pattern.

Crystallization: Long-range ordering of matter into regular structures, i.e., crystals, upon cooling from the melt.

Crystallization temperature: Temperature at which crystallization occurs.

Deconvolution: Fourier-transformation by which the total heat flow from MDSC is split into its reversing (RHF) and non-reversing heat flows (NRHF).

Endotherm: Positive change in enthalpy, i.e., absorption of heat, that accompanies melting.

Enthalpy relaxation: Endothermic loss of order that result from an increase in molecular mobility at the glass transition.

Exotherm: Negative change in enthalpy, i.e., release of heat, which accompanies crystallization or cold crystallization.

Glass transition temperature (T_g): The critical temperature at which amorphous matter goes from a hard and brittle state to being elastic and flexible, or vice versa. The transition is characterized by a change in relaxation time such that below T_g the relaxation times are long and molecular motions are reduced, whereas above T_g relaxation times are short and molecular motions are fast.

Melting: Disordering of crystalline matter into amorphous matter upon heating.

Modulated differential scanning calorimetry (MDSC): Method where a sinusoidal heating (cooling) is superimposed to the linear heating (cooling) of standard differential scanning calorimetry. The result is a modulation of the temperature that depends on the frequency and the amplitude of the cyclic signal.

Non-reversing heat flow (NRHF): Heat flow from molecular motions or processes that do not reach equilibrium within an MDSC modulation period. Non-equilibrium processes typically include oxidation, evaporation, decomposition, and chemical reactions.

Relaxation: Approach of steady-state after a change in the equilibrium condition.

Reversing heat flow (RHF): Heat flow from atomic motions responsible for the heat capacity, and from molecular processes rapid enough to occur during an MDSC modulation period.

Rigid amorphous material: Amorphous material whose molecular mobility is reduced by its association with adjacent crystalline material.